Int. J. Heat Mass Transfer. Vol. 22, pp. 1539–1546.

0017–9310/79/1101–1539 $02.00/0

THE EFFECT OF DISSIPATION ON FREE CONVECTION LOOPS

YORAM ZVIRIN*
Faculty of Mechanical Engineering, Technion, Israel Institute of Technology, Haifa, Israel

(*Received* 13 *October* 1978 *and in revised form* 7 *February* 1979)

Abstract—A theoretical evaluation is presented of the effect of dissipation on natural circulation loops, heated from below and cooled from above. A one dimensional model, wherein the only space coordinate runs along the loop, is applied to two types of loops: (I) two vertical branches with point heat source and sink, and (II) a toroidal loop heated by a uniform heat flux at the lower half and cooled by a constant wall temperature at the upper half.

It is found that for laminar flow in the first loop, dissipation affects only the temperature distribution but neither the steady state flow rate nor the stability characteristics. For laminar and turbulent flows in the second loop, the steady state velocities are enhanced by dissipation. Curves of marginal stability for various dissipation factors are given.

NOMENCLATURE

A, cross-sectional area;
a, coefficient in the expression for the friction coefficient f;
b, coefficient in the expression for the friction coefficient f;
C_i, constants of integration, equations (12) and (29);
c, specific heat;
D, dimensionless parameter for loop II, equation (20);
E, dimensionless parameter for loop II, equations (20, 21);
F, overall frictional parameter for loop I;
f, friction coefficient, $f = a/Re^b$;
g, acceleration of gravity;
h, heat transfer coefficient;
L, total length of loop I;
m, constant, equation (15);
n, constant, equation (15);
P, ratio of perimeter to cross sectional area;
Q, volumetric flow rate;
q, heat flux input;
R, major radius of torus (Fig. 2);
Re, Reynolds number;
r, (Hydraulic) radius of flow channel (minor radius of torus—Fig. 2);
S, total circulation length;
s, coordinate along the loop;
Δs, length of heat source (and heat sink);
T, temperature;
T_{ref}, reference temperature;
T_w, wall (or ambient) temperature;
ΔT, ΔT, (constant) wall temperatures at heat source and sink;
t, time;
U, characteristic velocity of loop II, equation (19);
V, mean velocity;
y, complex function, equation (30);
z, vertical coordinate.

Greek symbols

α, dimensionless parameter for loop I, equation (4);
β, thermal expansion coefficient;
ε, dimensionless parameter for loop I, equation (4);
θ, angular coordinate;
μ, dynamic viscosity;
ρ, density;
ρ_{ref}, reference density (at temperature T_{ref});
σ, stability parameter, equations (10), (26);
τ_w, wall shear stress;
Φ, dissipation function;
ϕ, dimensionless dissipation parameter, equation (5) for loop I or equation (21) for loop II.

Superscripts

$\bar{}$, steady state;
$\hat{}$, amplitude of the deviation from steady state.

1. INTRODUCTION

SOME geophysical phenomena as well as several engineering applications involve free convection loops where a fluid is heated from below and cooled from above. These loops appear in atmospheric and oceanic flows, in refrigeration cycles of the absorption type, in cryogenic systems and in the most commonly used system for solar energy utilization—the thermosyphon solar water heater. Shitzer *et al.* [1] investigated the performance of such a heater (140 liters storage tank, about 3 m^2 collector area) and measured at noontime on a clear summer day in

*Presently on a sabbatical leave at Electric Power Research Institute 3412 Hillview Avenue, Post Office Box 10412, Palo Alto, CA 94303, U.S.A.

Haifa, Israel (latitude 32°N) flow rates of the order of $1\,\mathrm{kg\,min^{-1}}$, associated with a temperature variation between 55 and 70°C along the collector. Keller [2] and Welander [3] treated analytically a loop consisting of two vertical branches with a point heat source and a point heat sink (Fig. 1). They investigated steady state behavior and oscillatory instability of it. Zvirin and Greif [4] investigated the transient behavior of this loop. Creveling *et al.* [5]

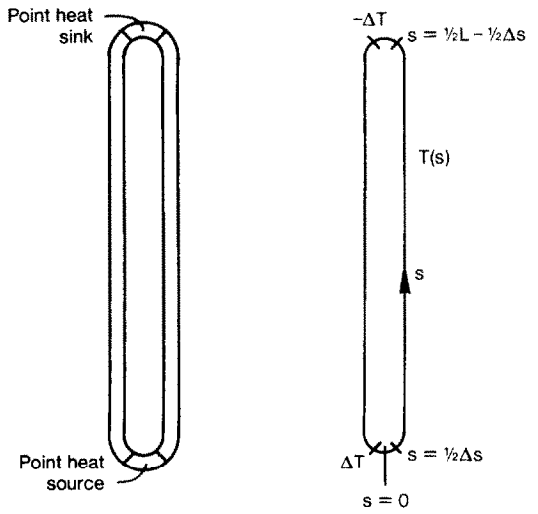

FIG. 1. The loop of two vertical branches with point heat source and sink.

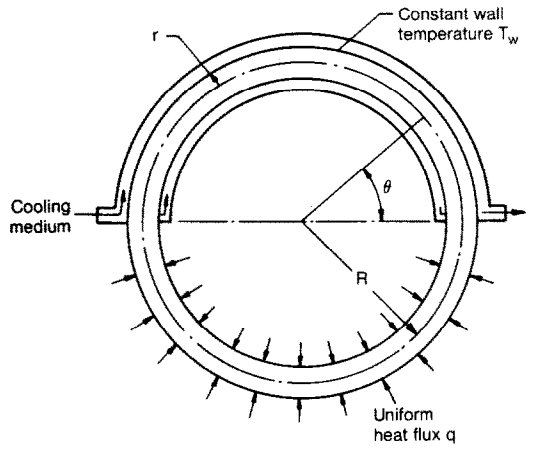

FIG. 2. The circular toroidal loop.

and Damerell and Scheonhals [6] studied experimentally and theoretically the instability of a circular loop (Fig. 2) caused by heating uniformly the lower half and cooling by constant wall temperature at the upper half. Ong [7] suggested a numerical method to evaluate the performance of the thermosyphonic solar water heater. Zvirin *et al.* [8, 9] have applied several analytical models for describing the steady state motion and instability characteristics of such solar heaters.

All the existing models for natural circulation loops do not take into account viscous heating of the fluid. The purpose of the present work is to study the effect of dissipation on free convection loops. Two systems are considered: (I), the two vertical branches (Fig. 1)—Section 2, and (II), the toroidal loop (Fig. 2)—Section 3. For laminar flow in the first system it is found that while the steady state temperature distribution is changed due to dissipation, the flow rate as well as the stability characteristics are not affected at all. For laminar and turbulent flows in the second system both temperature and flow rate at steady state are modified by viscous heating. The results of Creveling *et al.* [5] for the case where dissipation can be neglected are extended here by a more accurate solution. Finally, the effect of dissipation on the stability of the system is evaluated.

The models for natural convection loops are all one dimensional: the only space coordinate s runs along the circulation loop. The temperature T is thus the mean cross-sectional. Use is being made of the Boussinesq approximation wherein the density ρ is taken to be constant in the governing equations except for the buoyancy forces where $\rho = \rho_{\mathrm{ref}}[1-\beta(T-T_{\mathrm{ref}})]$; β is the thermal expansion coefficient and ρ_{ref} is the density at some reference temperature T_{ref}. According to these assumptions and the continuity equation, the flow rate Q is uniform along the loop at any time t.

The momentum equation is obtained by integration along the closed loop, thus the pressure terms vanish. Following Welander [3] and Creveling *et al.* [5], the resulting equation is:

$$\rho_0 \frac{\mathrm{d}V}{\mathrm{d}t} S = \rho_0 g\beta \oint T\,\mathrm{d}z - \oint P\tau_w\,\mathrm{d}s, \qquad (1)$$

where V is the mean velocity Q/A, A is the cross-sectional area, S is the circulation length, g the acceleration of gravity, z a vertical coordinate and P is the ratio of perimeter to cross-sectional area. The wall shear stress τ_w is expressed by $\tau_w = \frac{1}{2}f\rho(V\mu c)^2$, where $f = a/Re^b$. a and b depend on the flow regime and the Reynolds number is defined by $\rho_0 2rV/\mu$ where $2r$ is the (hydraulic) diameter and μ is the dynamic viscosity.

Neglecting axial heat conduction, the energy equation is written for each part of the system:

$$\rho c\left(\frac{\partial T}{\partial t} + V\frac{\partial T}{\partial s}\right) = Pq - Ph(T-T_w) + \frac{1}{A}\int \Phi\,\mathrm{d}A, \qquad (2)$$

where c is the specific heat of the fluid, q denotes heat flux input, h is a heat transfer coefficient, T_w the wall (or ambient) temperature and Φ is the dissipation function. The last term in equation (2) can be expressed as const $\cdot V^2$.

In the solutions for the two systems in Sections 2 and 3 it is assumed that the heat transfer coefficients, the fluid properties and the geometry (A and P) are constant. Dimensionless parameters will be defined separately for the two systems, to match Welander's [3] and Creveling's [5] notations.

2. THE TWO VERTICAL BRANCHES WITH POINT HEAT SOURCE AND SINK (LOOP I)

The loop consists of two insulated vertical branches of lengths $\frac{1}{2}L$. Small sections of lengths Δs at the bottom and top are heated and cooled by constant wall temperatures ΔT and $-\Delta T$ respectively (see Fig. 1). The heat transfer coefficients h there tend to infinity while $\Delta s \to 0$ in such a way that the heat addition remains finite (point source and point sink).

Following Welander [3], laminar flow is assumed where the shear stress at the wall depends linearly on the mean velocity (and on the flow rate). Equation (1) then takes the form:

$$\frac{dQ}{dt} = \frac{Ag\beta}{L}\oint T\,dz - FQ, \tag{3}$$

where F is a frictional coefficient. The parameters are made dimensionless by scaling lengths by $L/2$, time by $L/(2h\Delta s)$, temperature by ΔT and flow rate by $PhA\Delta s/(\rho c)$. (Note that $Ph/\rho c$ was denoted k by Welander.) The non-dimensional momentum equation is:

$$\frac{dQ}{dt} + \varepsilon Q = \tfrac{1}{2}\alpha\int_0^2 T\,ds, \tag{4}$$

where $\varepsilon = FL/(2h\Delta s)$ and $\alpha = g\beta\Delta TL/2(h\Delta s)^2$. The energy equation (2) for the insulated vertical branches takes on the following dimensionless form:

$$\frac{\partial T}{\partial t} + Q\frac{\partial T}{\partial s} = \phi Q^2. \tag{5}$$

ϕ is the dissipation coefficient; for a parabolic velocity profile, the definition of ϕ yields $\phi = \frac{1}{2}(\varepsilon/\alpha)(g\beta L/c)$. In Welander's [3] solution dissipation is ignored. There may be cases for which this term is not negligible, as can be seen by a calculation of ϕ.

The boundary conditions for the temperature distribution are obtained by considering the source and sink. Following, again, Welander [3], we get for $Q > 0$ at the source:

$$T_0 - T_2 = (1 - T_2)(1 - e^{-1/Q}), \tag{6a}$$

and at the sink:

$$T_{1+} - T_{1-} = -(1 + T_{1-})(1 - e^{-1/Q}), \tag{6b}$$

where $T_0 = T_{s=0+\Delta s/2}$; $T_{1-} = T_{1-\Delta s/2}$ etc.

When $\phi = 0$ the flow system is antisymmetric and only one branch and one boundary condition need be treated. Here the two branches must be considered. The steady state solution is derived by solving, first, equations (5) and (6) with $\partial T/\partial t = 0$, leaving $\bar{Q}$ as an unknown constant. The resulting temperature distribution is given by:

$$\bar{T} = \phi\bar{Q}\left(s + \frac{e^{-1/\bar{Q}}}{1 - e^{-1/\bar{Q}}}\right) + \frac{1 - e^{-1/\bar{Q}}}{1 + e^{-1/\bar{Q}}}, \qquad 0 < s < 1, \tag{7a}$$

$$\bar{T} = \phi\bar{Q}\left(s + \frac{2e^{-1/\bar{Q}} - 1}{1 - e^{-1/\bar{Q}}}\right) - \frac{1 - e^{-1/\bar{Q}}}{1 + e^{-1/\bar{Q}}}, \qquad 1 < s < 2. \tag{7b}$$

This steady state temperature distribution is shown schematically in Fig. 3. The steady state flow rate is obtained from equation (4), after performing the integral using (7). It is found that ϕ vanishes completely and the equation for $\bar{Q}$ is that obtained by Welander [3] for the case of no dissipation:

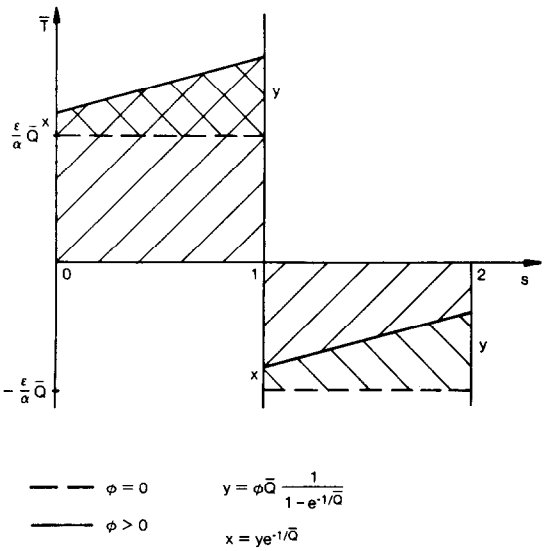

FIG. 3. The temperature distribution in the first loop.

$$\frac{\varepsilon}{\alpha}\bar{Q} = \frac{1 - e^{-1/\bar{Q}}}{1 + e^{-1/\bar{Q}}}, \tag{8a}$$

or

$$\frac{2\bar{Q}}{\alpha/\varepsilon + \bar{Q}} = 1 - e^{-1/\bar{Q}}. \tag{8b}$$

The vanishing of the dissipation terms from the buoyancy integral is illustrated in Fig. 3. Since the integral is the sum of the two areas between $\bar{T}$ and the s axis, it is seen that the same areas are added and subtracted by any $\phi > 0$ to those for $\phi = 0$.

The solution for $\bar{Q}$, depending on a single parameter α/ε, was obtained numerically by Welander [3]. We add here the asymptotic solutions for small and large values of α/ε:

$$\bar{Q} \to \alpha/\varepsilon \quad \text{as} \quad \alpha/\varepsilon \to 0, \tag{9a}$$

$$\bar{Q} \to \sqrt{\frac{1}{2}\frac{\alpha}{\varepsilon}} \quad \text{as} \quad \alpha/\varepsilon \to \infty. \tag{9b}$$

Stability of the steady state motion is analyzed by linearized stability equations. Writing the flow rate and temperature as:

$$Q(t) = \bar{Q} + \hat{Q}e^{\sigma t}, \qquad T(t, s) = \bar{T}(s) + \hat{T}(s)e^{\sigma t}, \tag{10}$$

where $\hat{Q}$ and $\hat{T}$ are small deviations, the perturbation equations derived from (4), (5) and (6) become (after subtracting the steady state equations):

$$(\sigma+\varepsilon)\hat{Q} = \tfrac{1}{2}\alpha \int_0^2 \hat{T}\,\mathrm{d}s, \tag{11a}$$

$$\bar{Q}\frac{\mathrm{d}\hat{T}}{\mathrm{d}s} + \sigma\hat{T} = \phi\bar{Q}\hat{Q}, \tag{11b}$$

$$\hat{T}_0 - \hat{T}_2\,\mathrm{e}^{-1/\bar{Q}} + \frac{1-\bar{T}_2}{\bar{Q}^2}\,\mathrm{e}^{-1/\bar{Q}}\hat{Q} = 0, \tag{11c}$$

$$\hat{T}_1 - \hat{T}_1\,\mathrm{e}^{-1/\bar{Q}} - \frac{1+\bar{T}_1}{\bar{Q}^2}\,\mathrm{e}^{-1/\bar{Q}}\hat{Q} = 0. \tag{11d}$$

In (11b) use was made of the steady state temperature distribution ($\mathrm{d}\bar{T}/\mathrm{d}s = \phi\bar{Q}$). This equation is solved for $\hat{T}(s)$ in terms of $\hat{Q}$:

$$\hat{T}_i = C_i\,\mathrm{e}^{-(\sigma/\bar{Q})s} + \frac{\phi\bar{Q}\hat{Q}}{\sigma}, \quad i = r, l, \tag{12}$$

r denotes the right branch, l the left one. Introducing (12) into (11a) to perform the integral, the following relation is obtained:

$$\hat{Q} = \frac{\alpha\bar{Q}}{2\sigma(\sigma+\varepsilon)}(1-\mathrm{e}^{-\sigma/\bar{Q}})(C_r - C_l\,\mathrm{e}^{-\sigma/\bar{Q}}). \tag{13}$$

The conditions (11c), (11d) yield, after using (12):

$$C_r - C_l\,\mathrm{e}^{-\sigma/\bar{Q}} = -\frac{2n}{1+m\,\mathrm{e}^{-\sigma/\bar{Q}}}\hat{Q}, \tag{14}$$

where

$$m = \mathrm{e}^{-1/\bar{Q}}, \quad n = \frac{\mathrm{e}^{-1/\bar{Q}}}{\bar{Q}^2}\left(1+\frac{\varepsilon}{\alpha}\bar{Q}\right), \tag{15}$$

and the definition of n is also based on (8a). The characteristic equation for σ is now obtained by introduction of (14) into (13):

$$1+m\,\mathrm{e}^{-\sigma/\bar{Q}} + \frac{n\alpha\bar{Q}}{\sigma(\sigma+\varepsilon)}(1-\mathrm{e}^{-\sigma/\bar{Q}}) = 0, \tag{16}$$

which is identical to that derived by Welander [3] for the case of no dissipation. (Note that m and n depend on $\bar{Q}$ only and thus are independent of ϕ.) Therefore, the solution of equation (16) and the curve of marginal stability obtained by Welander (in the $\varepsilon-\bar{Q}$ plane) hold for any value of ϕ.

It might seem surprising that dissipation does not have any effect on the stability of the system. However, the mechanism of instability, as explained by Welander [3] stems from phase shifts between the flow rate and buoyancy force. Apparently, the phase shift does not depend on ϕ for the system under consideration; note that the buoyancy integral and the steady state flow rate are independent of the dissipation term.

3. THE CIRCULAR LOOP, DISTRIBUTED HEATING AND COOLING (LOOP II)

The toroidal loop, shown in Fig. 2, was treated by Creveling *et al.* [5] without regarding dissipation effects. A uniform heat flux q is applied at the circumference of the lower half and the upper half wall temperature T_w is kept constant. According to the assumptions mentioned above, the momentum and energy equations (1) and (2) are:

$$\rho_W\frac{\mathrm{d}V}{\mathrm{d}t} = \frac{\rho_W\beta g}{2\pi}\int_0^{2\pi} T\cos\theta\,\mathrm{d}\theta - \frac{2}{r}\times\frac{1}{2}\,\rho_W a Re^{-b}V^2, \tag{17}$$

$$\rho_w c\left(\frac{\partial T}{\partial t} + \frac{V}{R}\frac{\partial T}{\partial\theta}\right) = \begin{cases} -\dfrac{2h}{r}T + \dfrac{2}{r^2}\displaystyle\int\Phi r'\,\mathrm{d}r', & 0<\theta<\pi, \\ \dfrac{2}{r}q + \dfrac{2}{r^2}\displaystyle\int\Phi r'\,\mathrm{d}r', & \pi<\theta<2\pi, \end{cases} \tag{18}$$

where T is the temperature above T_w. The boundary conditions are given by the continuity of the temperature distribution. Three cases will be considered; laminar flow with $a = 16$, $b = 1$, the other two based on the observations of Creveling *et al.* [5]: laminar flow with $a = 151$, $b = 1.17$ and turbulent regime with $a = 0.88$, $b = 0.45$, transition occurring at $Re \sim 1500$.

The parameters are made dimensionless by scaling temperature by q/h, velocity by U and time by $2\pi R/U$. U is a characteristic velocity, based on the approximate steady state solution obtained by Creveling *et al.*:

$$U = \left(\frac{2^{b+2}r^b\rho_w^{b-1}\beta g q R}{\pi a c\mu^b}\right)^{1/(3-b)} \tag{19}$$

The dimensionless form of equations (17) and (18) takes the form:

$$\frac{\mathrm{d}V}{\mathrm{d}t} = \frac{8\pi^2}{DE}\int_0^{2\pi} T\cos\theta\,\mathrm{d}\theta - \frac{32\pi}{E}V^{2-b}, \tag{20}$$

$$\frac{\partial T}{\partial t} + 2\pi V\frac{\partial T}{\partial\theta} = \begin{cases} -2DT+\phi V^2, & 0<\theta<\pi, \\ 2D+\phi V^2, & \pi<\theta<2\pi, \end{cases} \tag{21}$$

where $D = 2\pi Rh/\rho_W crU$, $E = 16rRe_{ch}^b/aR$, $Re_{ch} = 2r\rho_W U/\mu$ and for a parabolic velocity profile $\phi = 4Dg\beta R/\pi c$. It is noted that ϕ/D for laminar flows with a parabolic velocity profile would be very small (less than 10^{-3}) in a loop of the type investigated by Creveling *et al.* [5]. However, the value of this dissipation parameter will considerably increase for turbulent flows: moreover, according to the observations of Damerell and Schoenhals [6], the velocity profile is much more complicated, including regions of reversed flow. This would be associated with more viscous dissipation. Finally, since the parameter ϕ depends linearly on the thermal expansion coefficient β, the effects of dissipation will be most important in cryogenic applications, where β has relatively large values. It is well known, indeed, that in such flow applications, viscous dissipation must be taken into account.

The steady state solution procedure is similar to that used above. The temperature distribution is

obtained by integration of (21), taking into account the conditions $T(2\pi) = T(0)$, $T(\pi^-) = T(\pi^+)$:

$$T = \frac{2D+\phi\bar{V}^2}{2\bar{V}(1-e^{-D/\bar{V}})} e^{-\frac{D}{\bar{V}}\frac{\theta}{\pi}} + \frac{\phi\bar{V}^2}{2D}, \quad 0 \leqslant \theta \leqslant \pi, \quad (22a)$$

$$T = \frac{2D+\phi\bar{V}^2}{2\bar{V}}\left(\frac{\theta}{\pi}-1\right) + \frac{2D+\phi\bar{V}^2}{2\bar{V}} \frac{e^{-D/\bar{V}}}{1-e^{-D/\bar{V}}} + \frac{\phi\bar{V}^2}{2D}, \quad \pi \leqslant \theta \leqslant 2\pi. \quad (22b)$$

This distribution is introduced into (20), leading to the following equation for the steady state velocity $\bar{V}$:

$$\frac{2D+\phi\bar{V}^2}{\bar{V}}\left\{1+\frac{D(1+e^{-D/\bar{V}})}{2\bar{V}[1+(D/\pi\bar{V})^2](1-e^{-D/\bar{V}})}\right\} = 4D\bar{V}^{2-b}. \quad (23)$$

The solution of Creveling *et al.* [5] with no dissipation ($\phi = 0$) is an approximation for small D. The left hand side of (23) reduces then to $4D/\bar{V}$, hence $\bar{V} = 1$ and the steady state velocity is U.

A numerical solution of equation (23) yields the results shown in Fig. 4 for $\bar{V}$ as a function of D for various values of the ratio ϕ/D. It is seen that the approximation for small D is quite good when $D < 1$.

The asymptotic behavior of equation (23) for small and large D becomes:

$$2D+\phi\bar{V}^2 = 2D\bar{V}^{3-b}, \quad D \ll 1, \quad (24a)$$

$$2D+\phi\bar{V}^2 = 4D\bar{V}^{3-b}, \quad D \gg 1, \quad (24b)$$

and the asymptotic solutions for no dissipation are:

$$\bar{V} = 1, \quad D \ll 1, \quad \phi = 0, \quad (25a)$$

$$\bar{V} = (0.5)^{1/(3-b)} = \begin{cases} 0.707 & b = 1, \\ 0.685 & b = 1.17, \\ 0.762 & b = 0.45, \end{cases} \quad D \gg 1, \quad \phi = 0. \quad (25b)$$

These results are explained by the following reasoning: a large D can imply a large heat transfer coefficient h, causing smaller temperatures and therefore smaller buoyancy, hence also smaller velocities. If an increase in D is caused by a smaller value of the specific heat c, the results must be investigated more carefully: while the dimensionless velocity $\bar{V}$ decreases, the real velocity increases because c also appears in the definition of the characteristic velocity U. Indeed, a smaller specific heat would serve to increase temperature changes along the loop and thus to increase the buoyancy.

As can be seen from Fig. 4, dissipation tends to increase the steady state flow rate. This is explained by the following argument: the heat input of the source is a given constant; the effect of dissipation is a further temperature increase of the fluid. At steady state, this energy has to be transferred out by the circulating fluid, thereby increasing the flow rate in the loop. It can also be noticed that the additional energy (which can also be termed shear drag effect) is exactly equal to the work done by the gravitational field, expressed by $\oint \rho g \, dz$.

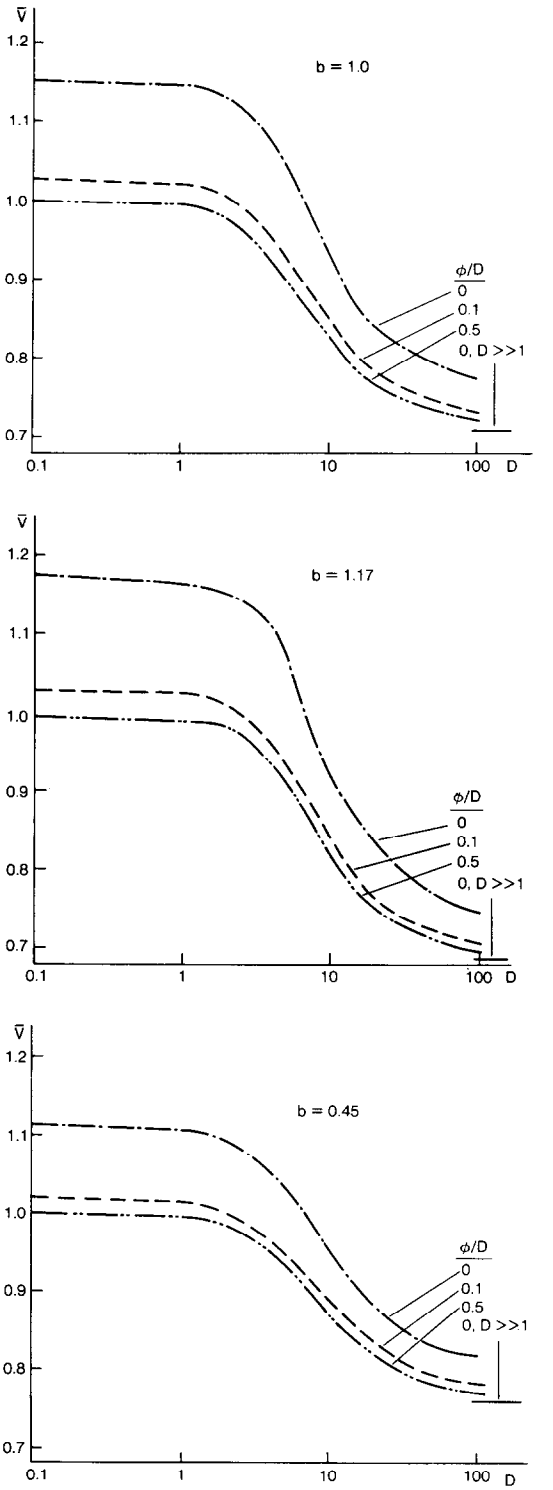

FIG. 4. The steady state velocity as a function of D and the dissipation parameter (second loop): a: laminar flow, $b = 1$; b: laminar flow, $b = 1.17$; c: turbulent flow, $b = 0.45$.

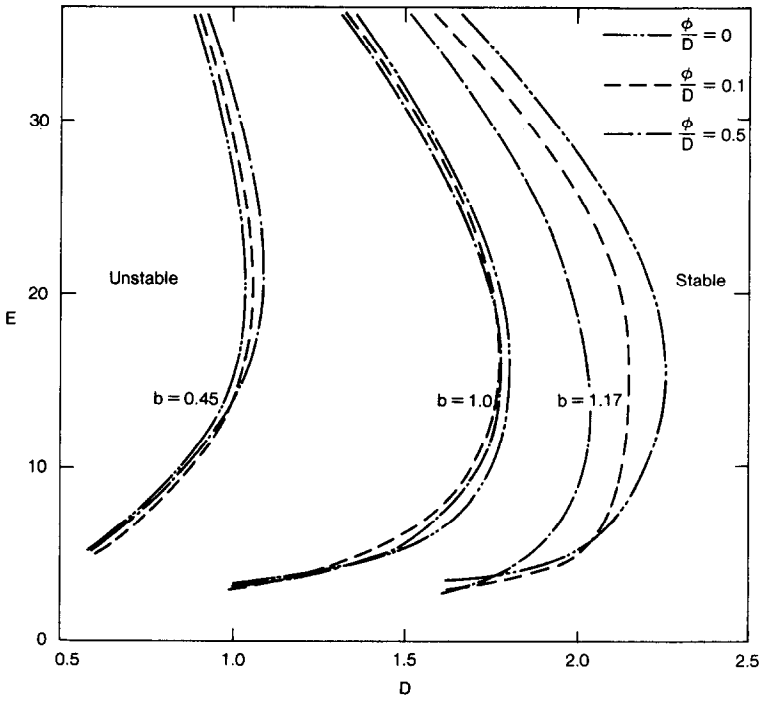

FIG. 5. Marginal stability curves in the E–D plane, for various dissipation parameters (second loop).

Stability of the steady state motion is analyzed by the same procedure used in Section 2. The velocity and temperature are written as:

$$V(t) = \bar{V} + \hat{V}e^{\sigma t}, \quad T(t,\theta) = \bar{T}(\theta) + \hat{T}(\theta)e^{\sigma t}, \tag{26}$$

where $\hat{V}$ and $\hat{T}$ are small perturbations. Introducing (26) into (20) and (21), linearizing the equations and substituting the steady state relations, the following perturbation equations are obtained:

$$\sigma\hat{V} = \frac{8\pi^2}{DE}\int_0^{2\pi}\hat{T}\cos\theta\,d\theta - \frac{32\pi}{E}\hat{V}, \tag{27}$$

$$\sigma\hat{T} + 2\pi\bar{V}\frac{d\hat{T}}{d\theta} + 2\pi\hat{V}\frac{d\bar{T}}{d\theta} = \begin{cases} -2D\hat{T} + 2\phi\bar{V}\hat{V}, & 0 < \theta < \pi, \\ 2\phi\bar{V}\hat{V}, & \pi < \theta < 2\pi. \end{cases} \tag{28}$$

Equations (28) are solved for $\hat{T}(s)$, using $d\bar{T}/d\theta$ from (22) and imposing the continuity conditions $\hat{T}(0) = \hat{T}(2\pi)$, $\hat{T}(\pi^-) = \hat{T}(\pi^+)$:

$$\frac{\sigma+2D}{2\bar{V}}\frac{\theta}{\pi} + \frac{D(2D+\phi\bar{V}^2)}{\sigma\bar{V}^2}\frac{1}{1-e^{-D/\bar{V}}}e^{-\frac{D}{\bar{V}}\frac{\theta}{\pi}} + \frac{2\phi\bar{V}\hat{V}}{\sigma+2D}, \quad 0 < \theta < \pi, \tag{29a}$$

$$T = c_2\hat{V}e^{-\frac{\sigma}{2\bar{V}}\frac{\theta}{\pi}} + \frac{\phi\bar{V}^2 - 2D}{\sigma\bar{V}}\hat{V}, \quad \pi < \theta < 2\pi, \tag{29b}$$

where

$$c_2 = \frac{1}{e^{D/\bar{V}} - e^{-\sigma/\bar{V}}} \times \left[\left(\frac{\phi\bar{V}-2D}{\sigma\bar{V}} - \frac{2\phi\bar{V}}{\sigma+2D}\right)\left(1-e^{-\frac{\sigma+2D}{2\bar{V}}}\right)\right] - \frac{D(2D+\phi\bar{V}^2)}{\sigma\bar{V}^2}\frac{1-e^{\sigma/2\bar{V}}}{1-e^{-D/\bar{V}}}, \tag{29c}$$

$$c_1 = c_2 e^{-\sigma/\bar{V}} + \frac{\phi\bar{V}^2-2D}{\sigma\bar{V}} - \frac{2\phi\bar{V}}{\sigma+2D} - \frac{D(2D+\phi\bar{V}^2)}{\sigma\bar{V}^2}\frac{1}{1-e^{-D/\bar{V}}}. \tag{29d}$$

The temperature distribution (29) is now used to perform the integral in (27) yielding the characteristic equation for σ:

$$y(\sigma) = c_1\frac{\frac{\sigma+2D}{2\bar{V}}\left(1+e^{-\frac{\sigma+2D}{2\bar{V}}}\right)}{1+\left(\frac{\sigma+2D}{2\pi\bar{V}}\right)^2} + \frac{D^2(2D+\phi\bar{V}^2)}{\sigma\bar{V}\left(\bar{V}^2+\frac{D^2}{\pi^2}\right)}\frac{1+e^{-D/\bar{V}}}{1-e^{-D/\bar{V}}} - c_2\frac{\frac{\sigma}{2\bar{V}}(e^{-\sigma/\bar{V}}+e^{-\sigma/2\bar{V}})}{1+\left(\frac{\sigma}{2\pi\bar{V}}\right)^2} - 4D\left(\frac{\sigma E}{32\pi}+1\right) = 0. \tag{30}$$

Curves of marginal stability (vanishing of the real part of σ) in the E–D plane are obtained from equation (30) by the Nyquist criterion in a method

similar to that of Creveling *et al.* [5]. The results are illustrated in Fig. 5, for the three cases discussed here: laminar flow with $a = 16$, $b = 1$, laminar flow with $a = 151$, $b = 1.17$ and turbulent flow with $a = 0.88$, $b = 0.45$*. As can be seen from the results, the effect of dissipation is not unique and it does not always make the flow more stable—i.e. the stable region in the D–E plane does not always enlarge with the dissipation parameter. In turbulent flow, the dissipation effect is mostly to decrease the stable zone. It is mentioned, again, that the mechanism of instability is rather complicated and is explained by the phase shift between the oscillations in the flow rate and buoyancy force. The dependence of this phase shift and therefore the marginal stability curves on the dissipation parameter is obviously not uni-directional.

Acknowledgements—The author is grateful to Mr. Danny Wolfshtein, who performed the numerical calculations, and to Professor R. Greif and Mr. A. Mertol for their helpful comments.

* It is noted that the marginal stability curve for laminar flow with $b = 1.17$ obtained here is somewhat different than that derived by Creveling *et al.* [5]. This difference follows from the approximation made in [5] leading to $\bar{V} = 1$. As mentioned above, the approximation is justified for $D < 1$; therefore, the marginal stability curve for turbulent flow (Fig. 5) which lies in this region, is identical with that of [5].

REFERENCES

1. A. Shitzer, D. Kalmanoviz, Y. Zvirin and G. Grossman, Experiments with a flat-plate solar water heating system in thermosyphonic flow, *Solar Energy* **22**, 27–35 (1979).
2. J. B. Keller, Periodic oscillations in a model of thermal convection, *J. Fluid Mech.* **26**, 599–606 (1966).
3. P. Welander, On the oscillatory instability of a differentially heated fluid loop, *J. Fluid Mech.* **29**, 17–30 (1967).
4. Y. Zvirin and R. Greif, Transient behavior of natural circulation loops: two vertical branches with point heat source and sink, *Int. J. Heat Mass Transfer* **22**, 499–504 (1979).
5. H. F. Creveling, J. F. De Paz, J. Y. Baladi and R. J. Schoenhals, Stability characteristics of a single-phase free convection loop, *J. Fluid Mech.* **67**, 65–84 (1975).
6. P. S. Damerell and R. J. Schoenhals, Flow in a toroidal thermosyphon with angular displacement of heated and cooled sections, ASME Paper 78-HT-44 (1978).
7. K. S. Ong, A finite difference method to evaluate the thermal performance of a solar water heater, *Solar Energy* **16**, 137–147 (1974).
8. Y. Zvirin, A. Shitzer and G. Grossman, The natural circulation solar heater-models with linear and nonlinear temperature distributions, *Int. J. Heat Mass Transfer* **20**, 997–999 (1977).
9. Y. Zvirin, A. Shitzer and A. Bartal-Bornstein, On the stability of the natural circulation solar heater, Proc. 6th Int. Heat Transfer Conference, Toronto, Canada Vol. 2, 141–145 (1978).

EFFET DE LA DISSIPATION SUR LES BOUCLES DE CONVECTION NATURELLE

Résumé—On présente une étude théorique de l'effet de la dissipation sur les boucles de convection naturelle chauffées à la base et refroidies au sommet. Un modèle monodimensionnel avec l'unique coordonnée d'espace suivant le parcours est appliqué à deux types de boucles: (I) deux branches verticales avec source et puits de chaleur ponctuels, et (II) un tore chauffé à flux uniforme à sa moitié inférieure et refroidi à température pariétale uniforme à la moitié supérieure. On trouve que, pour l'écoulement laminaire, dans la première boucle la dissipation affecte seulement la distribution de température sans modifier le débit permanent ni les caractéristiques de stabilité. Dans la seconde boucle, aussi bien pour les écoulements laminaires que turbulents, les vitesses en régime permanent sont augmentées par la dissipation. On donne des courbes de stabilité marginale pour différents facteurs de dissipation.

DER EINFLUSS DER DISSIPATION AUF FREIE KONVEKTIONSWALZEN

Zusammenfassung—Eine theoretische Berechnung des Dissipationseinflusses auf von unten beheizte und von oben gekühlte natürliche Konvektionswalzen wird dargestellt. Ein eindimensionales Modell, bei dem die einzige Raumkoordinate entlang der Walze verläuft, wird auf zwei Typen von Walzen angewandt: (I) zwei vertikale Zweige mit punktförmiger Wärmequelle und Senke und (II) eine ringförmige Walze, die durch einen gleichförmigen Wärmestrom in der unteren Hälfte beheizt und bei konstanter Wandtemperatur in der oberen Hälfte gekühlt wird. Es zeigt sich, daß bei laminarer Strömung in der ersten Walze Dissipation nur die Temperaturverteilung, aber weder die stationäre Massenstromdichte noch das Stabilitätsverhalten beeinflußt. Bei laminaren und turbulenten Strömungen in der zweiten Walze werden durch Dissipation die stationären Geschwindigkeiten vergrößert. Es werden für verschiedene Dissipationsfaktoren Kurven der Grenzstabilität angegeben.

ВЛИЯНИЕ ДИССИПАЦИИ В КОНТУРАХ СО СВОБОДНОЙ КОНВЕКЦИЕЙ

Аннотация — Представлен теоретический расчет влияния диссипации на естественную циркуляцию в нагреваемых снизу и охлаждаемых сверху контурах. Одномерная модель, в которой пространственная координата направлена вдоль контура, используется для расчета двух типов контуров: (I) два вертикальных канала с точечным источником и стоком тепла, и (II) торроидальный контур, нагреваемый за счет равномерного подвода тепла к нижней половине контура и охлаждаемый вследствие наличия постоянной температуры стенки в его верхней части.

Найдено, что при ламинарном потоке в первом контуре диссипация оказывает влияние только на распределение температур, но не влияет ни на скорость стабилизированного течения, ни на устойчивость течения. В случае ламинарного и турбулентного потоков во втором контуре скорость стабилизированного течения возрастает за счет диссипации. Представлены нейтральные кривые устойчивости при различных коэффициентах диссипации.